J Fluoresc
DOI 10.1007/s10895-015-1693-z

ORIGINAL ARTICLE

# Cd-Cysteine Nanorods as a Fluorescence Sensor for Determination of Fe (III) in Real Samples

**Ebrahim Ghiamati**[1] · **Ramin Boroujerdi**[1]

Received: 29 April 2015 / Accepted: 14 October 2015


**Abstract** A new Cd-Cysteine complex nanorods (Cd-Cys NRs) were synthesized in one step at room temperature, and its morphology, structure and spectral properties were characterized by transmission electron microscopy (TEM), elemental analysis (EA), X-Ray diffraction (XRD), solid state and normal UV-Vis, Fourier transform infrared (FTIR) and spectrofluorometry. The developed Cd-Cys NRs were used as a fluorescence sensor for detection of Fe (III) in different aqueous matrices. The selectivity and sensitivity of the fabricated nano-sensor based on its fluorescence quenching in the presence of Fe (III) were probed according to the Stern-Volmer equation. The detection limit of the method was in micromolar per liter range. Cd-Cys NRs response tested in different complex samples such as Rosemary plant leaves, exhibited a well-defined response. Anticoagulation measurements were performed to evaluate their blood biocompatibility.

**Keywords** Biosensor · Fluorescent probe · Cd-Cys nanorods · Fe(III) determination · Heavy metal ions · Hemocompatibility

## Introduction

Fluorescence sensing is a rapidly developing field of research and technology. Designing and synthesizing a selective and sensitive metal ion fluorescent sensor has attracted attention of chemists in the past two decades. Many attempts have been made to develop fluorescent probes for a variety of analytes due to fluorometric advantages such as ultimate sensitivity, specificity, simplicity, versatility, and high temporal and spatial resolution [1–7].

Iron ions can be found in almost everything around us, in water, soil, plants, foods, medicines, cells and so on [8–14]. Two physiochemical form of iron are well known, Fe (II) and Fe (III) which could be converted to each other through their environments like oxidation-reduction or pH changes. In the human body, Fe(II) is the form which utilizes in cell for oxygen storage and Fe(III) acts as active center of many enzymes [15]. Also Fe(II) can affect wine oxidation and its aging whereas Fe(III) capable of promoting precipitation in wine which is an example of the importance of measuring iron in industry [16].

Many techniques for the detection iron metal ions have been reported including electrochemical methods like voltammetry [17], and spectroscopic methods such as flame atomic absorption spectrometry (FAAS) [18], inductively coupled plasma mass spectrometry [19], inductively coupled plasma-atomic emission spectrometry (ICP-AES) [20] and spectrophotometric methods. Reported spectrophotometric methods usually suffer from several problems like working just in high acidic or basic solutions [21], long sensor synthesizing processes [22] or high cost of reagents [23].

Due to the uniqueness structure of biomolecules, the biomolecule-assisted methods in synthesizing of nanomaterials are promising and growing field of study [24–26]. Biological thiols, such as cysteine (Cys) and homocysteine (Hcy), play essential role in human physiology. Cys is a source of sulfide in iron sulfur clusters [27, 28]. Cys with -SH, $-NH_2$, and -COOH functional

**Electronic supplementary material** The online version of this article (doi:10.1007/s10895-015-1693-z) contains supplementary material, which is available to authorized users.

✉ Ebrahim Ghiamati
eghiamati@yahoo.com

[1] Department of Chemistry, Faculty of Science, University of Birjand, Birjand, Iran

Published online: 30 October 2015

groups has a strong tendency to coordinate with metal ions [24]. Positive effect of the capping of the luminescent CdS quantum dots (QDs) with Cys has been investigated with spectrofluorometric methods by Rosenzweig and Chen; capped QDs showed quenching in presence of Cu(II) and Fe(III) metal ions and enhanced by Zn(II) ions in water [29].

Moreover, one-dimensional semiconductor nanostructures such as nanorods (NRs) and nanowires (NWs) due to their special structures, unique electrical and optical properties have found their ways to analytical chemistry [30–33]. Many types of NRs or NR-based materials have been used as sensors, including metal oxide NRs such as ZnO and $W_2O_3$, polymer NRs and metal NRs such as Au nano-sensor [34]. In this research, Cd-Cys NRs, which were not reported before, were successfully synthesized with a convenient, one step method at room temperature. In presence of Fe (III), in aqueous solutions, synthesized NRs showed a significant fluorescence quenching at 363 nm ($\lambda_{ex}$ = 316 nm).

## Experimental

### Reagents

All chemicals were purchased from E. Merck, Darmstadt, Germany, and were of analytical reagent grade. Distilled deionized water (DDW) were used for preparing all of the solutions. The metal ions stock solutions of $1.0 \times 10^{-2}$ M were made up of their nitrate and chloride salts. The Hg (II) ions stock solutions of $1.0 \times 10^{-2}$ M were made up of their acetate salt.

### Instrumentation

Photoluminescence (PL) spectra were obtained using a Shimadzu RF-5301PC spectrofluorometer (Japan) in room temperature (298 ± 2 K). FTIR spectra were obtained by Thermo Nicolet Nexus 670 (USA). Absorption spectra were measured on double beam Analytik Jena Specord Plus spectrophotometer and solid phase UV-Visible spectra were acquired with Analytik Jena Specord S600 spectrophotometer. The morphology of the synthesized nanomaterials was probed by CM-philips10 transmission electron microscopy (TEM). PANalytical model X'Pert Pro MPD was used for acquiring XRD patterns. Gallenkamp muffle furnace (England) was employed for turning the plant leaves into ashes. Elementar model Vario EL III (Germany) used for Elemental Analysis. AA-6300 Shimadzu (Japan) atomic absorption spectrometer (AAS) was ultilized for measuring the amount of iron in the complex matrixes. Euronda sonicator model 4D (Italy) was used for dispersing the NRs in the water. For centrifugation, Hettich zentrifuge model D-78, 532 tuttlingen were utilized. All pH measurements were made with a Istek pH-220 L model equipped with a Istek USA built electrode. Wisettir model MSH-20D used for magnetic stirring of the solutions.

### Software

Drawing all of the chemical reactions and purposed three dimensional molecular structures was performed by using Chem & Bio 3D Ultra version 11.0 and Chem & BioDraw Ultra version 11.0 of CambridgeSoft products.

### Preparation of Complex Samples

*Feroglobin Medicine Tonic*

Feroglobin medicine made in Alborz Darou Company of Iran under the license of Vitobiotics Company of England used for this experiment. 1 mL of the tonic was diluted in a 1 L volumetric flask and was assayed by AAS. The amount of each ingredients has been taken from its bottle label and placed in Table 1.

*Synthesis of Cd-Cys NRs*

0.090 g of L-Cysteine and 0.230 g of $CdCl_2.H_2O$ were placed in 1 L beaker which contained 650 mL DDW and

**Table 1** Feroglobin medicine continents

| NO. | Nutrition information | Av. Per 5 mL | %RDA |
|---|---|---|---|
| 1 | Thiamin HCL (Vitamin B1) | 5 mg | 286 |
| 2 | Vitamin B2 | 1 mg | 63 |
| 3 | Vitamin B6 | 1 mg | 100 |
| 4 | Vitamin B12 (Cyanocobalamin) | 5 μg | 500 |
| 5 | Folic Acid | 50 μg | 75 |
| 6 | Dexpanthenol | 2 mg | – |
| 7 | Calcium Glycerophosphate | 10 mg | – |
| 8 | Nicotinamide (Vitamin B3) | 10 mg | 44 |
| 9 | Iron (Elemental) | 10 mg | 50 |
| 10 | Zinc (Elemental) | 3 mg | 33 |
| 11 | Vitamin C | 32 mg | – |
| 12 | Copper | 0.2 mg | – |
| 13 | Manganese | 0.25 mg | – |
| 14 | Lysine HCl | 20 mg | – |
| 15 | Honey | 100 mg | – |
| 16 | Malt Extract | 500 mg | – |

*RDA* recommended daily allowance

dissolved while it stirred with a magnetic stirrer and a glassy solution appeared. Then 4 mL of ethanolamine was added to the solution, the light cloudy solution was kept under stirring for 6 h using the speed of about 830 rounds per minute (RPM) at room temperature. The obtained white Cd-Cys $NR_s$ sediment separated from the solution by centrifugation, washed with absolute ethanol three times and dried at room temperature (Fig. 1). The synthesizing process was repeated for several times and the sediments were characterize each time with FTIR, UV-Vis and spectrofluorometer to make sure of the Cd-Cys NRs synthesizing process. The yield was about 88 %.

*Fluorescence Measurements*

0.080 g of the synthesized Cd-Cys NRs was dispersed in DDW by sonication, then transferred to 100 mL volumetric flask and diluted to the mark. Its fluorescence intensity was measured at 363 nm ($\lambda_{ex}$ = 316 nm) with 1- cm sample cell and slit width of 5.0 nm in fast scan mode. In further studies regarding fluorescence response of the Cd-Cys NRs, metal ion solutions or complex sample solutions was mixed equally with the 0.80 g/L Cd-Cys NRs solution. The Cd-Cys NRs florescence response was examined using the well-known Stern-Volmer equation (Eq. 1) and their corresponding plots.

$$\frac{F_0}{F} = 1 + K_{SV}\{Q\} \quad (1)$$

Where $F_0$ and F are Fluorescence intensity in the absence and presence of the quencher, $K_{SV}$ is the Stern–Volmer quenching constant, and Q is the concentration of the quencher.

## Results and Discussion

### Characterization of NRs

*TEM Image*

Figure 2 illustrates TEM images of the Cd-Cys NRs complex in 200 nm scale. As shown in the images the diameter range of Cd-Cys NRs are from 46 to 76 nm, their length is from 380 to 580 nm. The length is proportional to the diameter and thicker NRs are longer.

*XRD Pattern*

To find out crystalline or amorphous nature of the Cd-Cys NRs, a XRD pattern was acquired. The Cu anode was employed with scan speed of 2° per minute from 0 to 80°. As it is obvious from Fig. 3, unlike the amorphous form of Cd-Cys NWs [36], sharp and clear peaks proved its crystalline form. By comparing the Cd-Cys NRs XRD pattern with cysteine chloride which was reported by Jason G. Parsons et al. [37], the appearance of Cys peaks at 19, 21, 22 and 25° in the

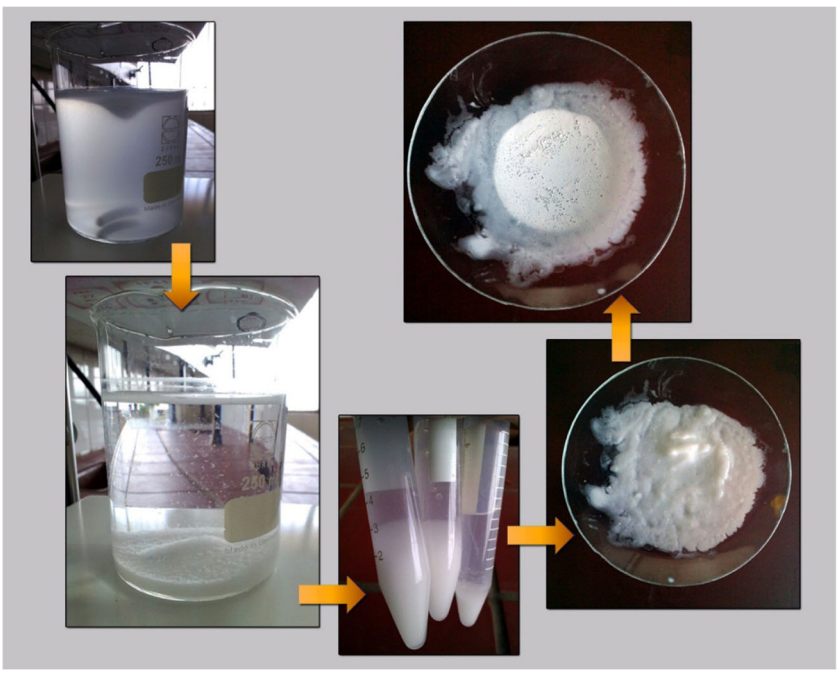

**Fig. 1** Schematic procedure of synthesizing NRs

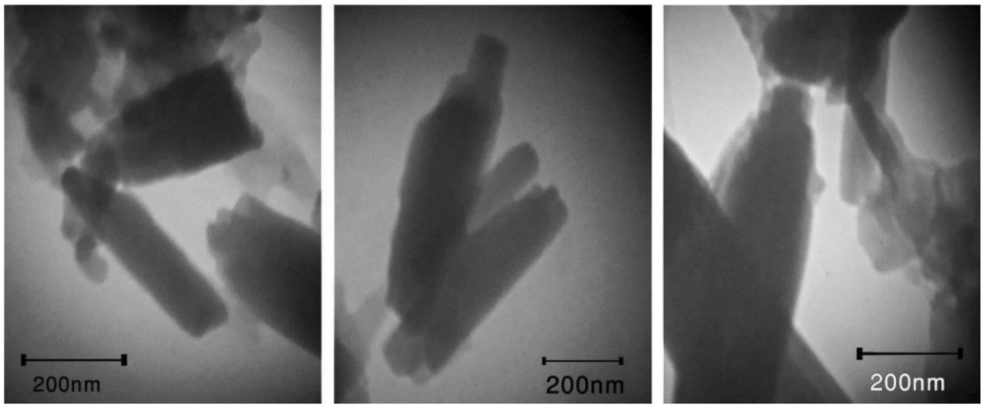


**Fig. 2** TEM images of Cd-Cys NRs

XRD patterns of Cd-Cys NRs, indicates the incorporation of Cys in the nanocomplex.

Using Scherrer equation (Eq. 2), the nano crystalline size (D) was calculated by the information on the XRD patterns.

$$D = \frac{K\lambda}{\beta \cos\theta} \tag{2}$$

Where $\lambda$ is radiation wavelength, β is full-width at half maximum, K is shape factor. Assuming the K = 0.90, the approximate diameter of the Cd-Cys NRs found to be 98.93 nm which is close enough to TEM results. The discrepancy between the theoretical value of NRs diameter and the measured diameter using TEM, comes from some inaccuracy in the Eq. 2 formula [38].

*FTIR Spectra*

A KBr pellet of Cys was prepared, and its FTIR spectrum was acquired. Characteristic vibrational frequencies of Cys were assigned in Fig. 4. Cys has three susceptible functional groups able to bind to cadmium ion.

Figure 5 is the FTIR spectra of Cd-Cys NRs, demonstrating the existence of two peaks at 3327 and 3255 $cm^{-1}$ which belong to primary amines, indicating the presence of N-H bond. The assumption that cadmium binds to $–COO^-$ group has been ruled out due to the presence of a strong peak at 1596 $cm^{-1}$. The absence of S-H peak from 2540 to 2600 $cm^{-1}$ shows that the binding between Cd and Cys has been occurred via –SH group of Cys.

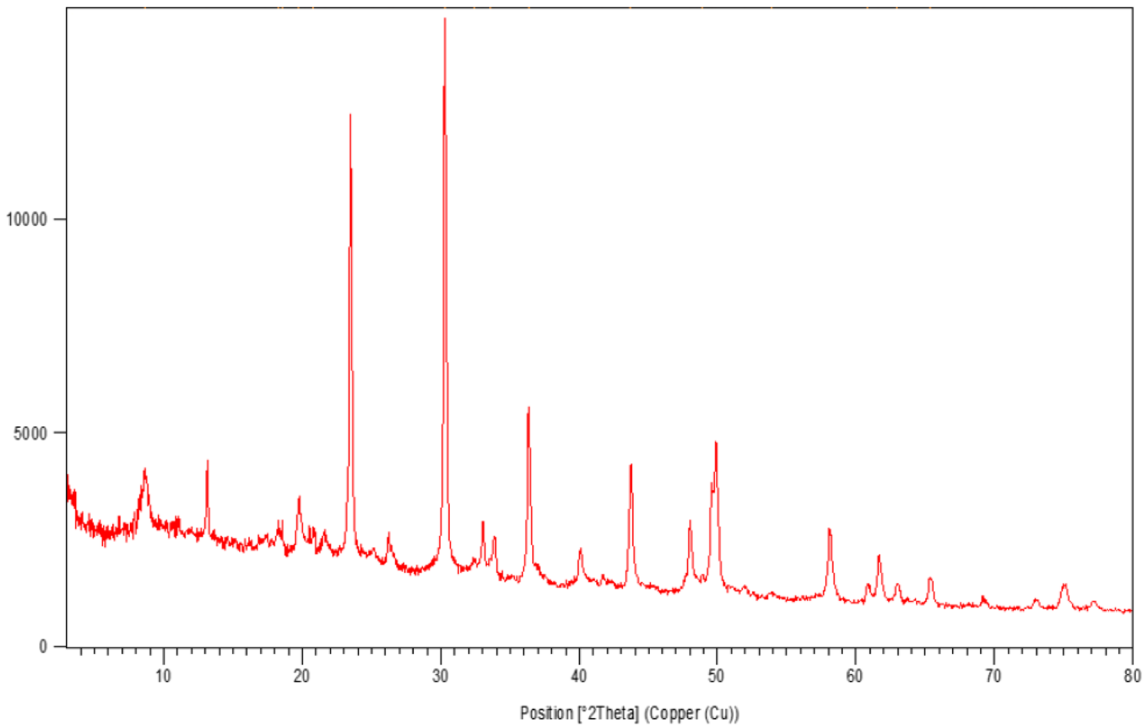


**Fig. 3** XRD pattern of Cd-Cys NRs

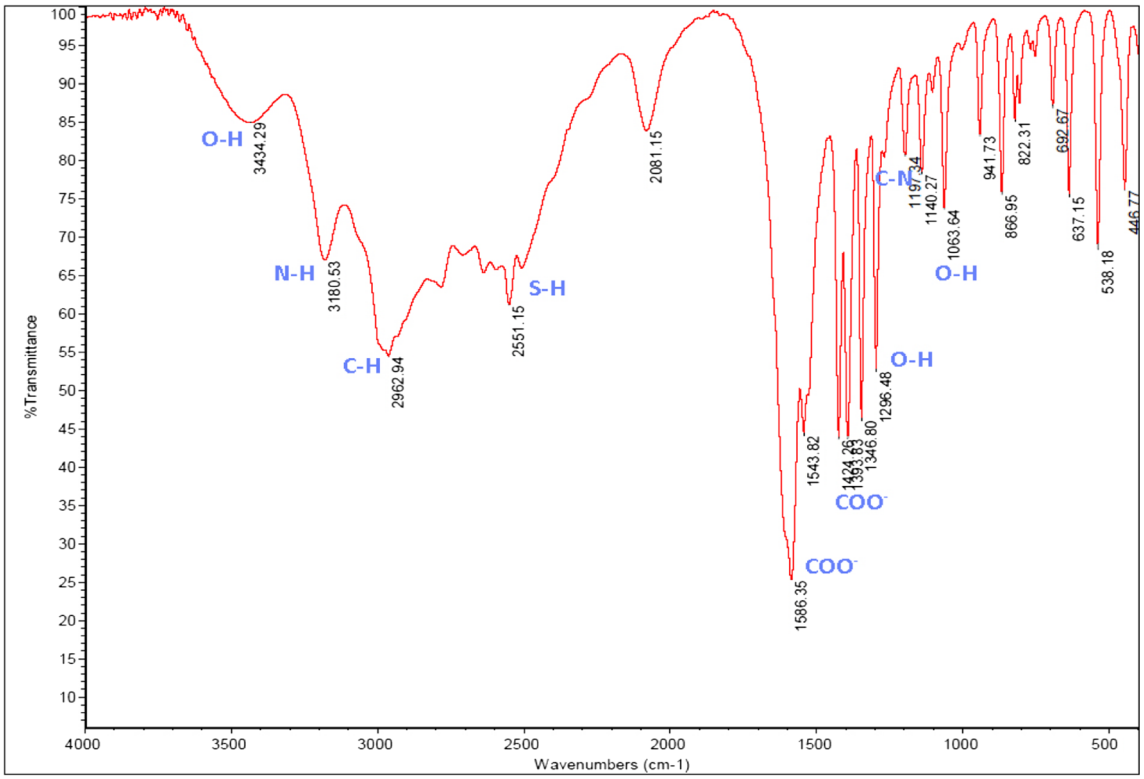


**Fig. 4** FTIR spectrum of L-Cysteine

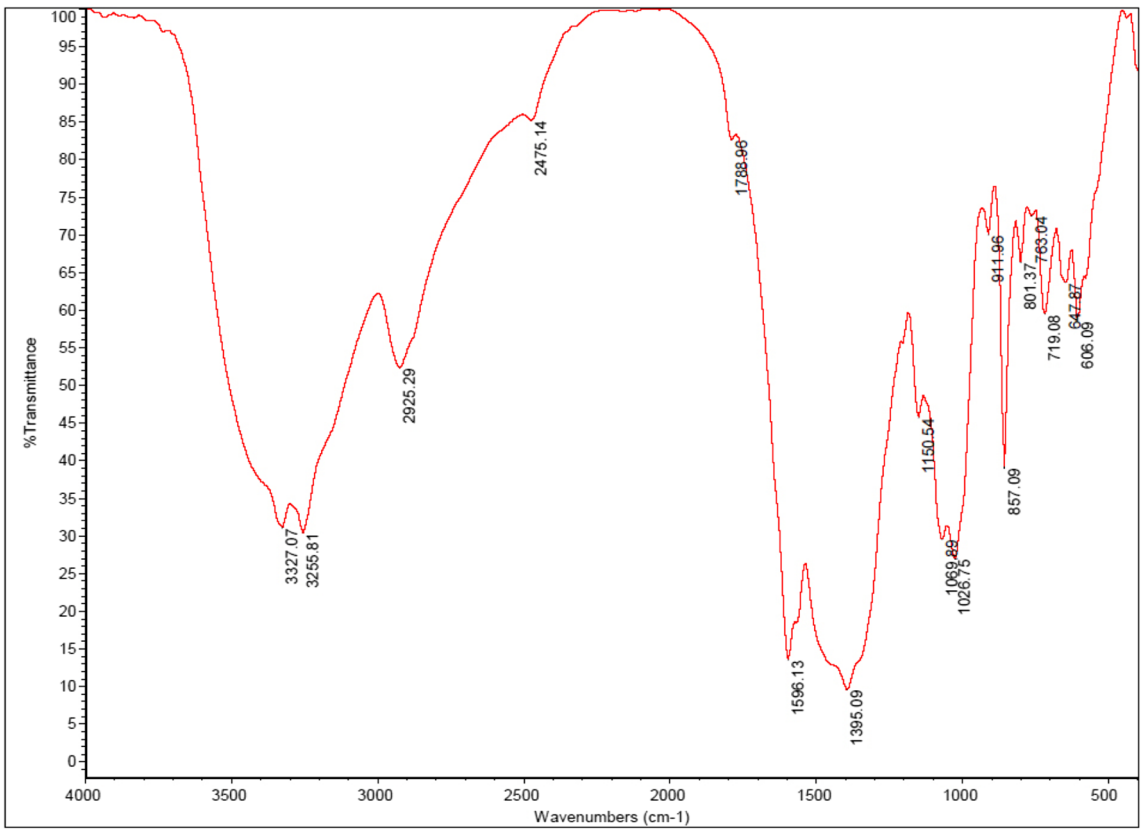


**Fig. 5** FTIR spectrum of NRs

*Normal UV-Vis Spectra*

Substantial information can be obtained by UV-Visible especially about molecular structure and identification [39]. Spectrophotometric technique could be used for molecular spectral characterization as well [40]. Three $10^{-4}$ mol/L solutions of Cd(II), Fe(III), Cys and a 0.8 g/L solution of Cd-Cys NRs were prepared in DDW and scanned through wavelengths range of 190 to 1000 nm. Little absorption in UV range was observed for Cd-Cys NRs (Fig. 6).

*Elemental Analysis*

By comparing to the other reports regarding similar structures for rod-like nanoparticles, $HOOCCH(NH_2)CH_2S$–Cd–OH molecular structure was purposed [24, 36, 41], which later was confirmed by elemental analysis as shown in Table 2.

On the basis of experimental results and possible Cd-Cys complexes structure [37], the purposed formation mechanism of Cd-Cys NRs is shown in Fig. 7. First Cys molecules have tendency to be attracted to the $Cd^{2+}$ ions by their –SH and $-NH_2$ groups which leads to the formation of Cd-S bond causing a primary complex of Cd-Cys comes to exist in water. After addition of ethanolamine which creates a weakly basic environment, metal-Cys NRs complex produces. The coordination reaction happening between Cd metal ions and –SH group of Cys causes uniform distribution of inorganic ions in the matrix.

**Table 2** Elemental analysis of Cd–Cysteine complex nanorods

| | Content % | | |
|---|---|---|---|
| | N | C | H |
| Experimental | 4.197 | 15.49 | 3.14 |
| Calculated | 5.60 | 14.44 | 2.83 |

**Effect of Temperature and NRs Concentration on the Fluorescence Emission**

Monitoring Cd-Cys NRs fluorescence emission intensity in temperature range of 10–65 °C (283–338 K) did not show any measurable changes (Figure S1) indicating insensitivity of the nano-sensor towards temperature fluctuations. Varying the Cd-Cys NRs concentration affected the intensity of the peaks, by increasing the concentration of Cd-Cys NRs from $5.00 \times 10^{-4}$ g/L to 1.10 g/L a remarkable rise in intensity of the fluorescence peak was observed (Fig. 8).

**Effect of pH on NRs Fluorescence Emission**

Very small amount of Cd-Cys NRs were taken for pH testing (about 0.05 g/L). Increasing the pH to 10 caused an increase in Cd-Cys NRs fluorescence emission, further increase did not

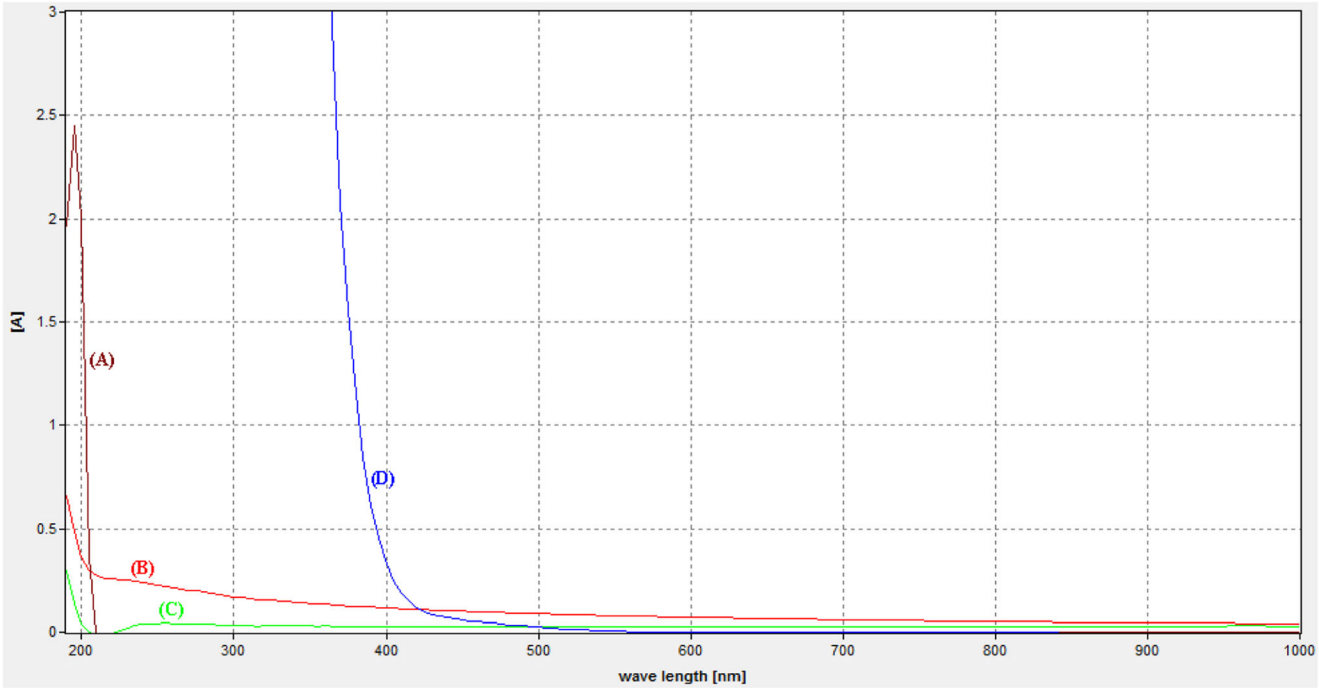


**Fig. 6** UV-Vis spectra: (*A*) is $Cd^{2+}$ solution, (*B*) is nanorods, (*C*) is L-Cysteine and (*D*) is stand for Fe(III) solution

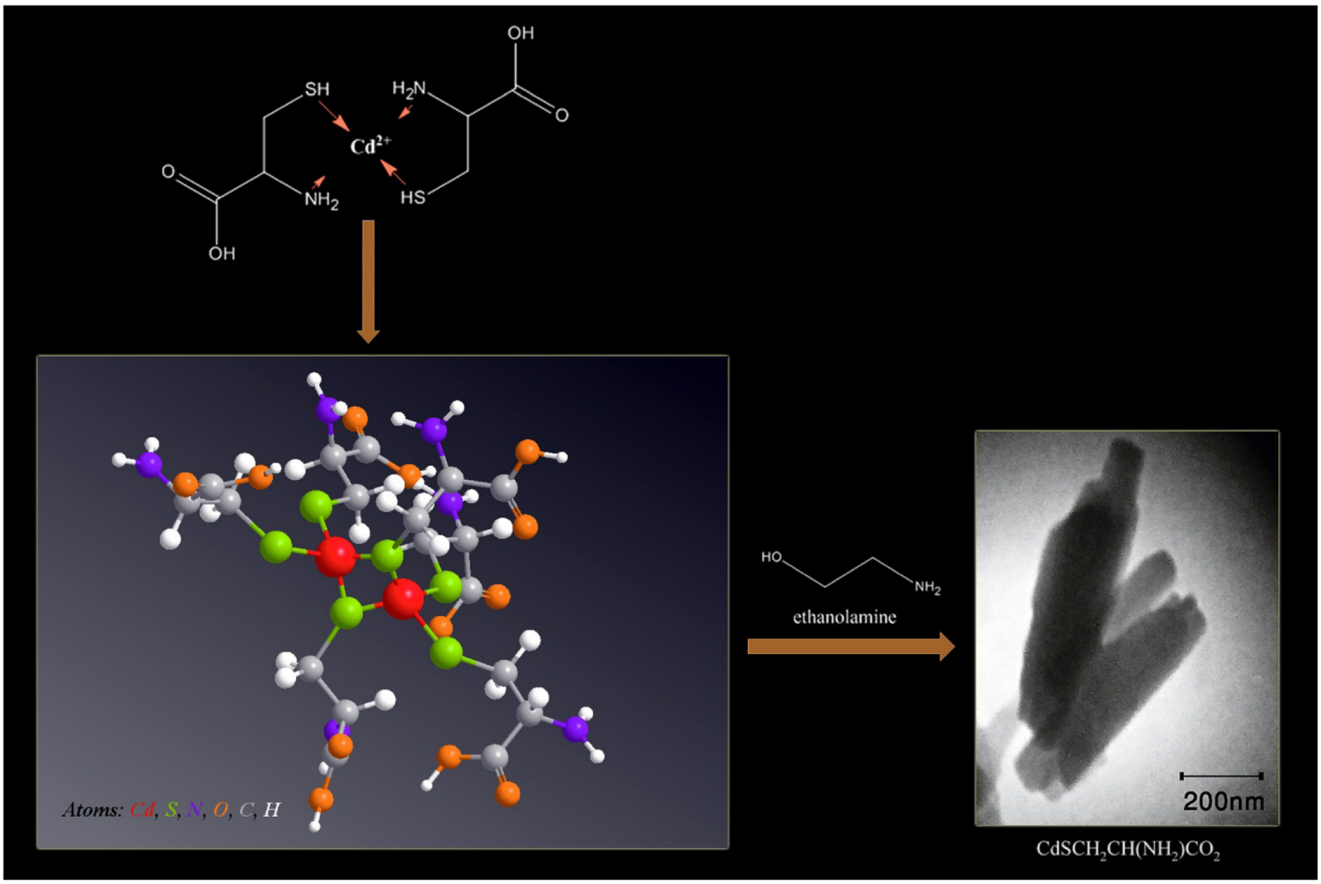


**Fig. 7** The scheme for the formation of Cd-Cys nanorods

lead to meaningful changes in the intensity of the peaks (Fig. 9). For choosing optimum pH, two more important points besides the peak intensity of Cd-Cys NRs in DDW should be considered. i) Further investigation shows that

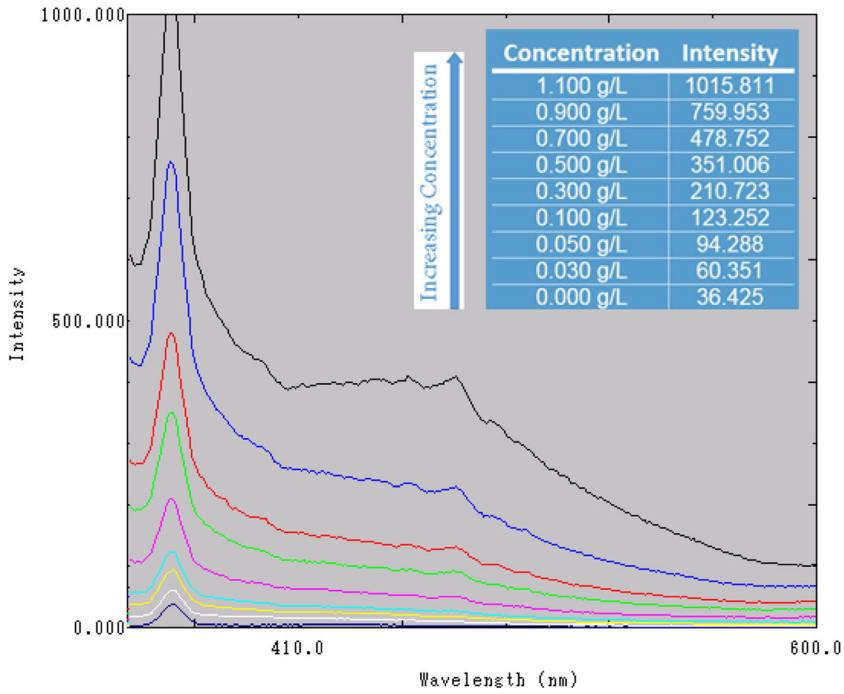


**Fig. 8** Effect of NRs concentration on the fluorescence peak

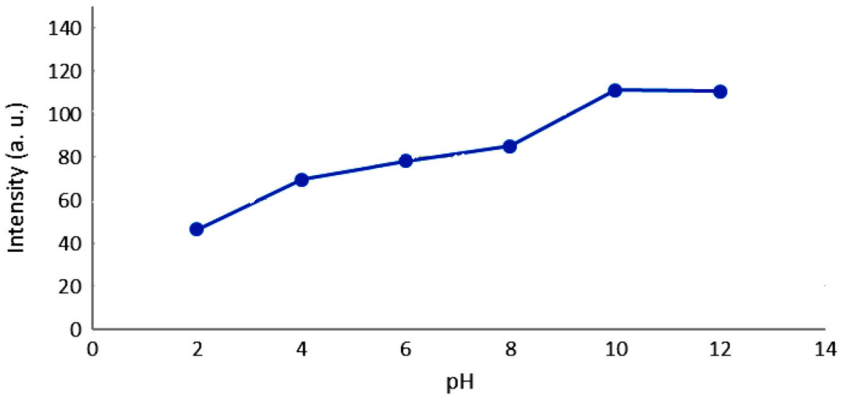


**Fig. 9** Effect of pH on solo NRs emission in DDW

increasing the pH to higher than 6.5 causes a decrease in the selectivity of Cd-Cys NRs in complex samples. ii) The changes in the degree of formation of different metal complexes in higher pHs could lead to co-precipitation of NRs with insoluble complexes or low soluble metal complexes, so pH of 6.5 was chosen as optimum pH.

## Effect of Different Metal Ions on NRs Fluorescence Emission

Two important parameters in chemical analysis, i.e. selectivity and sensitivity, of Cd-Cys NRs were investigated. Effects of 17 different metal ions ($Mg^{2+}$, $Na^{+}$, $Zn^{2+}$, $Al^{3+}$, $Mn^{2+}$, $K^{+}$, $Cd^{2+}$, $Hg^{2+}$, $Ag^{+}$, $Co^{2+}$, $Ni^{2+}$, $Ca^{2+}$, $Pb^{2+}$, $Cu^{2+}$, $Ce^{3+}$, $Fe^{2+}$, $Fe^{3+}$) on NRs fluorescence emission intensity were probed. The response of the Cd-Cys NRs toward Fe (III) ions was significantly more intense than the other metal ions showing a good selectivity. In fact there was no obvious change in fluorescence response for the other metal ions, except for $Cu^{2+}$, $Mn^{2+}$ and $Al^{3+}$ which is still so much weaker than response of the Cd-Cys NRs to the Fe(III) ions even at higher concentrations (Fig. 10).

Increasing the Fe(III) ions concentration in Cd-Cys NRs solution from $1.00 \times 10^{-8}$ mol/L to $1.00 \times 10^{-2}$ mol/L range caused the fluorescence emission intensity to quench (Fig. 11). There is a correlation between the ratios of fluorescence intensity versus concentration of Fe(III) over a wide range from $1.00 \times 10^{-7}$mol/L to $5.00 \times 10^{-4}$mol/L (Figure S2). The detection limit (DL) of the sensor could be calculated from the following equation:

$$DL = \frac{3S_b}{m}$$

Where $S_b$ is standard deviation and m is the slope of the curve. The detection limit was found to be $2.69 \times 10^{-7}$ mol/L.

## Mechanism of Quenching and Reaction Between NRs and Fe (III) Ions

### *Solid Phase UV-Vis Spectra*

As mentioned before, structural differences between the compounds can be characterized by UV-Visible spectroscopy.

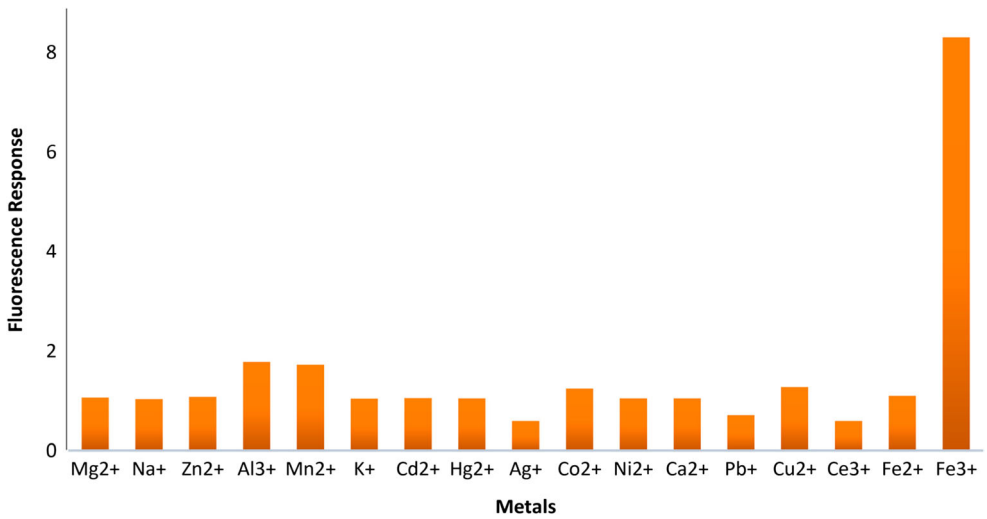


**Fig. 10** Fluorescence Response of Cd-Cys NRs to different metal ions. All metals have concentration of $1.00 \times 10^{-3}$ mol/L (pH = 6.5)

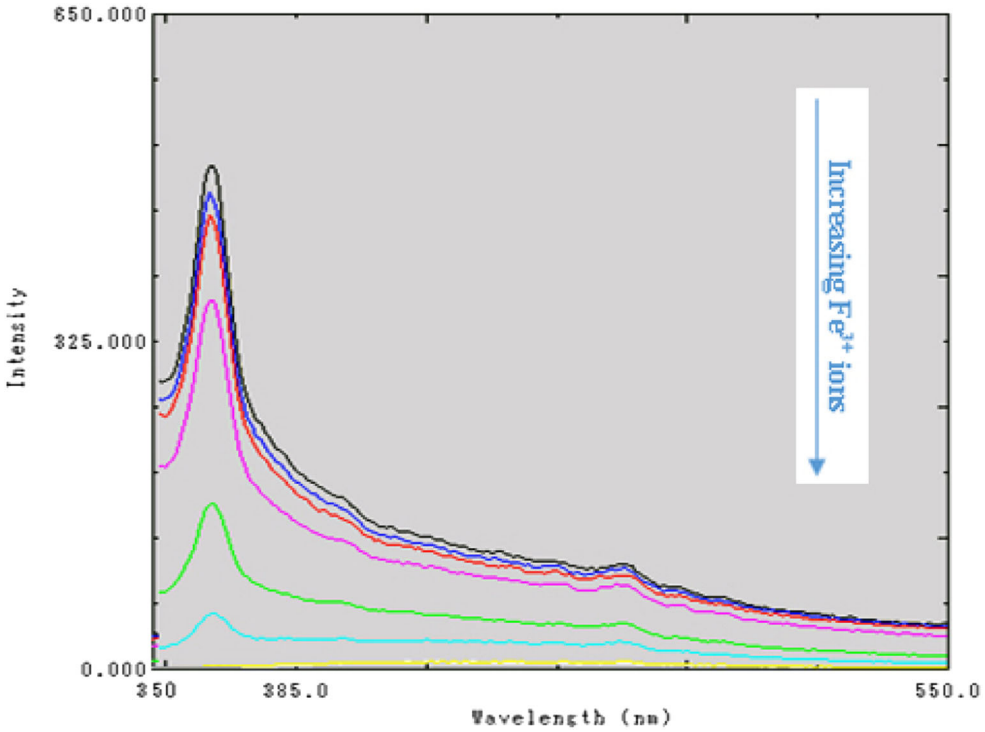


**Fig. 11** Effect of increasing Fe(III) ions on the NRs fluorescence emission intensity

About 10 mL of solution containing 0.5 g/L of Cd-Cys NRs in the presence of $10^{-4}$ mol/L of Fe (III) solution was prepared, dried and stored. A thin layer of Cd-Cys NRs solid and a thin layer of dried solid Cd-Cys-Fe complex placed in the cells respectively for taking their solid state UV-Vis spectrum from 200 to 1000 nm to compare their structures. As shown in the Fig. 12 there is a significant differences between the absorbance of the solo-nanorods (A) and nanorods in the presence of Fe (III) in the solution (B) proving structural changes and creation of a new complex.

*Normal UV-Visible Spectra*

As Doak et al. showed for gold nanoparticles [42], larger absorbance is related to larger particles in size distribution. The increase in absorbance of Cd-Cys NRs in the presence of $10^{-4}$ mol/L Fe (III) as shown in Fig. 13 is an evidence for creation of larger particles.

*FTIR Spectra*

Figure 14 exhibits the FTIR spectrum of Cd-Cys NRs reacted with Fe(III). Stored dried Cd-Cye-Fe complex used for acquiring the spectrum. Peaks at 3430 and 1034 $cm^{-1}$ belong to O-H. Peaks at 1596 and 1402 $cm^{-1}$ prove the presence of free $COO^-$ in the structure. Lack of the –SH group peak is due to bond formation between the Cd and Cys as Cd-S-R, but the absence of any peak for $–NH_2$ group shows that Fe(III) binds to the NRs structure making Fe-N-R bond.

The coordination bond between –SH and Cd(II) leads to the ligand to metal charge transfer. In the presence of Fe (III) metal ions, Fe (III) binds to $–NH_2$ groups of Cys. The intrinsic paramagnetism of Fe (III) metal ions is responsible for fluorescence quenching [42–46]. One of the possible reactions between NRs and Fe (III) is formation of a dative bond between non-bonding orbital electrons of nitrogen and empty orbital of Fe (III).

## Complex Matrix Samples

For testing the ability of the purposed nano-sensor in measuring the amount of analyte in real samples, three different industrial, biological and medicinal samples have been studied. AAS was chosen in two of real samples to compare our purposed fluorometric method precision with other spectroscopic methods.

*Artificial Wastewater*

Fe (III) ions have been used in wastewater treatment in co-precipitation process. Ni(II), Zn(II), Cu(II), Pb(II), Cd(II) are the common metals which could be removed from wastewater by Fe(III) salts like $FeCl_3$ [43, 44]. For studying the effect of these metal ions and their co-precipitation with Fe(III) on nano-sensor response an experiment was designed. A

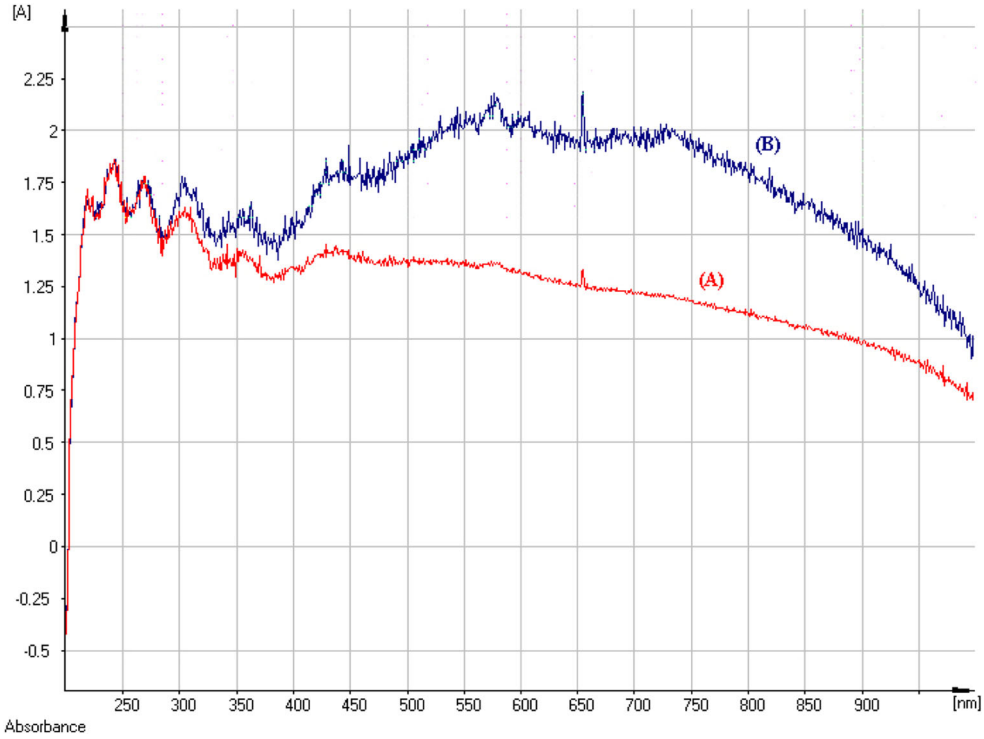


**Fig. 12** Solid state UV-visible spectra of (*A*): solo-nanorods and (*B*): nanoroads in the presence of Fe(III)

250 mL solution which contained $5.00 \times 10^{-5}$ mol/L of the above mentioned ions and $1.00 \times 10^{-4}$ mol/L of Fe (III) was made. NRs fluorescence response showed the concentration of $9.51 \times 10^{-5}$ mol/L (5 % error). The response of the detector indicated that Fe (III) ions had a priority for reaching the nano-sensor in comparision with the other metal ions.

*Rosmarinus officinalis Plant*

Different plants and herbs have been used and studied for long time as a flavor in foods or their healing abilities. Rosemary (Rosmarinus officinalis) is one of the well-known herbs with pharmacological and antimicrobial properties [45, 46]. In an

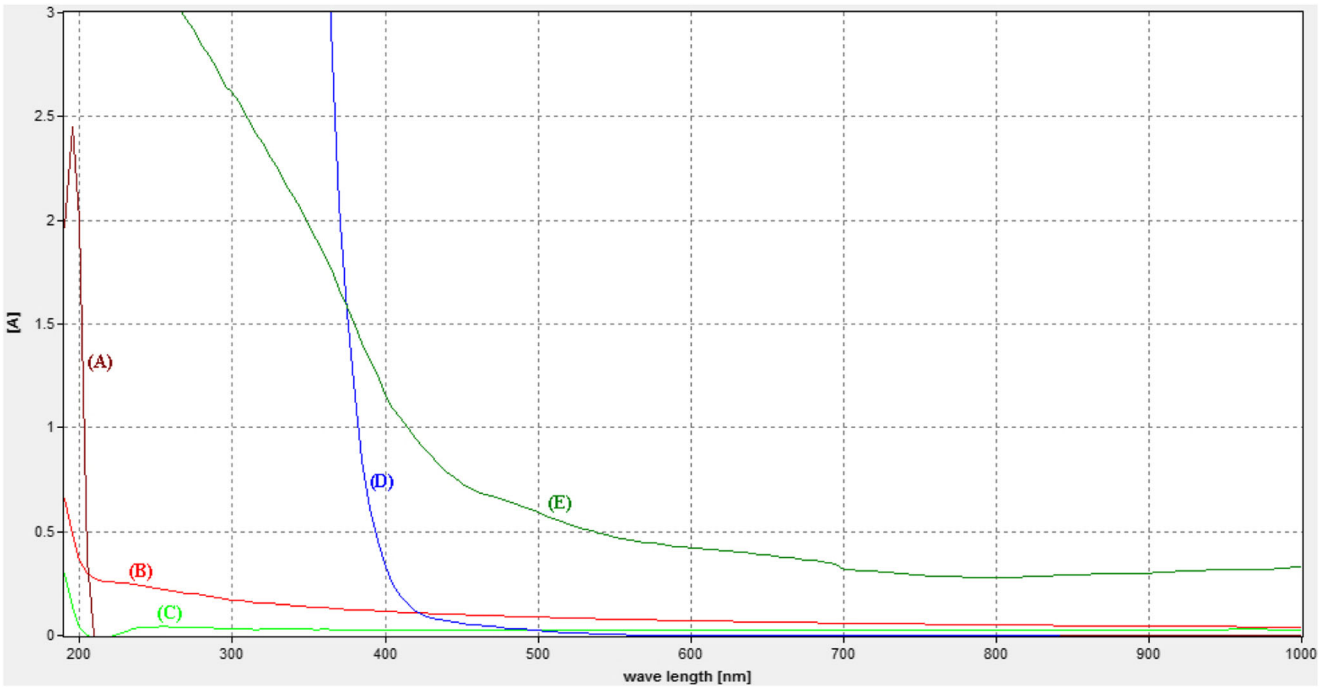


**Fig. 13** UV-visible spectras: (*A*) is $Cd^{2+}$ solution, (*B*) is nanorods, (*C*) is L-Cysteine, (*D*) is Fe(III) solution and (*E*) is blog to Cd-Cys-Fe complex

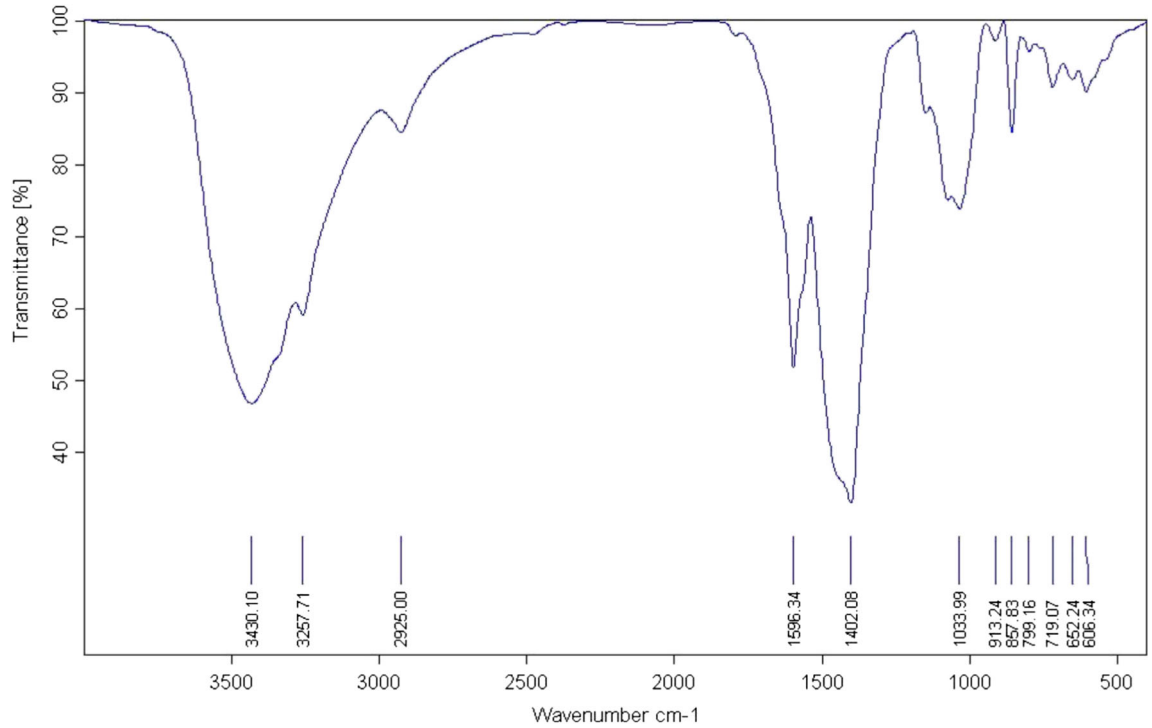


**Fig. 14** FTIR spectrum of Cd-Cys NRs reacted with Fe(III)

experiment the amount of iron was measured by the Cd-Cys nano-sensor. The leaves solution contains various different mineral metals plus iron, with different unknown concentrations. First the total amount of iron in the main solution was measured with AAS and found to be $1.35 \times 10^{-1}$ mol/L in the main solution. For setting the concentration on the linear range of the detector and testing its ability in measuring low amounts of analyte, 1 mL of the leaves solution was diluted in a 1 L volumetric flask to obtain $1.35 \times 10^{-4}$ mol/L concentration. The fluorescence response of the Cd-Cys NRs showed the concentration of Fe(III) in the solution was $7.1 \times 10^{-6}$ mol/L. Then one drop of $H_2O_2$ was added to the fluorescence cuvette containing the solution and the response of the Cd-Cys NRs gave Fe(III) concentration of $1.23 \times 10^{-4}$ mol/L (which has about 8 % error comparing to AAS response). This concentration will be the total amount of the iron in the solution because all of the Fe(II) was converted to Fe(III) according to the following equation:

$$H_2O_2 + 2H^+ + 2Fe^{2+} \rightarrow 2\,H_2O + 2Fe^{3+}$$

By subtraction of first response of the Cd-Cys NRs from the second one, we were able to measure the amount of the $Fe^{2+}$ in the solution which was $1.159 \times 10^{-4}$ mol/L.

*Feroglobin Medicine*

A Feroglobin medicine tonic known as specific blood building nutrient, contains ferrous sulfate in a complex with B vitamins, folic acid, minerals such as zinc which are also important in blood formation and other nutritional supplements. Here the amount of iron in this tonic was measured by Cd-Cys NRs fluorescence response. First the total amount of iron was determined with AAS and found to be $1.86 \times 10^{-1}$ mol/L in the main solution. For setting the concentration on the linear range of the detector, 1 mL of the main solution was diluted in a 1 L volumetric flask to obtain $1.86 \times 10^{-4}$ mol/L solution. The fluorescence response of the Cd-Cys NRs gave the value of Fe(III) $6.74 \times 10^{-6}$ mol/L; this amount of Fe(III) in the solution is near detection limit of the detector. Then one drop of $H_2O_2$ (35 %) was added to the cuvette. The concentration of Fe(III) was determined spectrofluorometrically and found to be $1.73 \times 10^{-4}$ mol/L (almost 6 % error with respect to AAS response). The second reading was the total concentration of iron in the solution because all of Fe(II) was converted to Fe(III). By subtracting the first response from the second, the amount of the Fe(II) found to be $1.66 \times 10^{-4}$ mol/L.

**Table 3** The APTT, PT, TT data

| | PT | APTT | TT |
|---|---|---|---|
| Plasma | 15.4 | 45 | 18.9 |
| NRs | 39.8 | 135.3 | 20.4 |

Reported PT, APTT and TT times are the average datum of the 10 times repeating the same testing

### Hemocompatibility Tests

High selectivity of the sensor makes it suitable candidate for biological and biochemical studies, such as measuring the amount of an analyte in blood, but selectivity itself is not enough; Hemocompatibility is a key property of biomaterials that comes in contact with blood [47]. Even in vitro blood analyses, sensor should not cause coagulation of the blood samples.

The in vitro anticoagulation activity of the Cd-Cys NRs was evaluated by prothrombin time (PT), activated partial thromboplastin time (APTT), and thrombin time (TT). The PT is corresponding to the extrinsic pathway of the blood-clotting system, APTT detects the intrinsic coagulation, and TT is the assay for the last step of coagulation, are well-known methods to determine the biocompatibility of the material [35, 48, 49]. All assays were conducted using citrated human plasma from a healthy donor. The results was shown in Table 3. Both the PT and APTT values are remarkably prolonged for Cd-Cys NRs with respect to plasma, indicating their significance in vivo anticoagulation activity. Clot time of APTT is considerably above the maximal values, almost three times greater compared to 45 s for plasma. A small increase is also detected for the TT value. The data in Table 3 exhibited a good blood compatibility of Cd-Cys complex NRs.

## Conclusion

We successfully synthesized and characterized new Cd-Cys NRs in one step at room temperature. Cd-Cys NRs which were utilized as a fluorescence nano-sensor complied with the most important characteristics of a favorable sensors that is stability, selectivity, sensitivity by measuring micro-molar per liter Fe (III) concentrations. The structure of the Cd-Cys NRs in the absence and presence of Fe (III) was examined. The hemocompatibility tested by anticoagulation measurements showed the biocompatibility of synthesized nano-sensors. The ability and response of the nano-sensor tested in different real samples with complex matrices and the results exhibited the usability of this method in pharmacological, phytochemical and industrial researches.

**Acknowledgments** We would like to thank Mr. Bahman Mansouri Motlagh for his special helps on anticoagulation measurements and blood sample analyzing, and University of Birjand Research Council for financial support.

## References

1. Jung HS, Han JH, Pradhan T, Kim S, Lee SW, Sessler JL, Kim TW, Kang C, Kim JS (2012) A cysteine-selective fluorescent probe for the cellular detection of cysteine. Biomaterials 33(3):945–953
2. Kim JS, Quang DT (2007) Calixarene-derived fluorescent probes. Chem Rev 107(9):3780–3799
3. De Silva AP, Gunaratne HN, Gunnlaugsson T, Huxley AJ, McCoy CP, Rademacher JT, Rice TE (1997) Signaling recognition events with fluorescent sensors and switches. Chem Rev 97(5):1515–1566
4. Jung HS, Kwon PS, Lee JW, Kim JI, Hong CS, Kim JW, Yan S, Lee JY, Lee JH, Joo T (2009) Coumarin-derived Cu2+—selective fluorescence sensor: synthesis, mechanisms, and applications in living cells. J Am Chem Soc 131(5):2008–2012
5. Neupane LN, Park J-Y, Park JH, Lee K-H (2013) Turn-on fluorescent chemosensor based on an amino acid for Pb (II) and Hg (II) ions in aqueous solutions and role of tryptophan for sensing. Org Lett 15(2):254–257
6. Han A, Liu X, Prestwich GD, Zang L (2014) Fluorescent sensor for $Hg^{2+}$ detection in aqueous solution. Sensors Actuators B Chem 198:274–277
7. Zhong K, Cai M, Hou S, Bian Y, Tang L (2014) A simple benzimidazole based fluorescent sensor for ratiometric recognition of Zn2+ in water. Bull Kor Chem Soc 35(2):489
8. Hu SH, Liu DM, Tung WL, Liao CF, Chen SY (2008) Surfactant-free, self-assembled PVA-iron oxide/silica core–shell nanocarriers for highly sensitive, magnetically controlled drug release and ultra-high cancer cell uptake efficiency. Adv Funct Mater 18(19):2946–2955
9. Kawakubo S, Hagihara Y, Honda Y, Iwatsuki M (1999) Speciation of iron in river and tap waters by catalytic spectrophotometry using oxidation of *o*-phenylenediamine with hydrogen peroxide. Anal Chim Acta 388(1):35–43
10. Niazi A, Zolgharnein J, Davoodabadi MR (2007) Simultaneous determination of aluminium and iron with hematoxylin using spectrophotometric and orthogonal signal correction-partial least squares in plant and water. Ann Chim 97(11–12):1181–1190
11. Brinkmann M, Teuffel R, Laham N, Ehrlich R, Decker P, Lemonnier FA, Pascolo S (2007) Expression of iron transport proteins divalent metal transporter-1, Ferroportin-1, HFE and transferrin receptor-1 in human monocyte-derived dendritic cells. Cell Biochem Funct 25(3):287–296
12. Locatelli C (2004) Heavy metals in matrices of food interest: sequential voltammetric determination at trace and ultratrace level of copper, lead, cadmium, zinc, arsenic, selenium, manganese and iron in meals. Electroanalysis 16(18):1478–1486
13. Unnithan MR, Vinod V, Anirudhan T (2002) Ability of iron (III)-loaded carboxylated polyacrylamide-grafted sawdust to remove phosphate ions from aqueous solution and fertilizer industry wastewater: adsorption kinetics and isotherm studies. J Appl Polym Sci 84(13):2541–2553
14. Hunt RC, Davis AA (1992) Release of iron by human retinal pigment epithelial cells. J Cell Physiol 152(1):102–110
15. Safavi A, Abdollahi H (2002) Simultaneous kinetic determination of Fe (III) and Fe (II) by H-point standard addition method. Talanta 56(4):699–704
16. Costa RCC, Araújo AN (2001) Determination of Fe (III) and total Fe in wines by sequential injection analysis and flame atomic absorption spectrometry. Anal Chim Acta 438(1):227–233
17. van den Berg CM (2006) Chemical speciation of iron in seawater by cathodic stripping voltammetry with dihydroxynaphthalene. Anal Chem 78(1):156–163
18. Andersen JE (2005) A novel method for the filterless preconcentration of iron. Analyst 130(3):385–390
19. Arnold GL, Weyer S, Anbar A (2004) Fe isotope variations in natural materials measured using high mass resolution multiple collector ICPMS. Anal Chem 76(2):322–327
20. Huber JK (1999) Determination of Cu, Fe, Mn, and Zn in blood fractions by SEC-HPLC-ICP-AES coupling. Analyst 124(5):657–663

21. Singh N, Kaur N, Dunn J, MacKay M, Callan JF (2009) A new fluorescent chemosensor for iron (III) based on the β-aminobisulfonate receptor. Tetrahedron Lett 50(8):953–956
22. Mao J, He Q, Liu W (2010) An rhodamine-based fluorescence probe for iron (III) ion determination in aqueous solution. Talanta 80(5):2093–2098
23. Tripathy SK, Woo JY, Han C-S (2013) Colorimetric detection of Fe (III) ions using label-free gold nanoparticles and acidic thiourea mixture. Sensors Actuators B Chem 181:114–118
24. Liu X-L, Zhu Y-J (2009) A precursor nanowire templated route to CdS nanowires. Mater Lett 63(12):1085–1088
25. Xiong S, Xi B, Xu D, Wang C, Feng X, Zhou H, Qian Y (2007) L-cysteine-assisted tunable synthesis of PbS of various morphologies. J Phys Chem C 111(45):16761–16767
26. Xiang J, Cao H, Wu Q, Zhang S, Zhang X, Watt AA (2008) L-cysteine-assisted synthesis and optical properties of Ag2S nanospheres. J Phys Chem C 112(10):3580–3584
27. Chen X, Zhou Y, Peng X, Yoon J (2010) Fluorescent and colorimetric probes for detection of thiols. Chem Soc Rev 39(6):2120–2135
28. Lill R, Mühlenhoff U (2006) Iron-sulfur protein biogenesis in eukaryotes: components and mechanisms. Annu Rev Cell Dev Biol 22:457–486
29. Chen Y, Rosenzweig Z (2002) Luminescent CdS quantum dots as selective ion probes. Anal Chem 74(19):5132–5138
30. Tang Z, Kotov NA, Giersig M (2002) Spontaneous organization of single CdTe nanoparticles into luminescent nanowires. Science 297(5579):237–240
31. Yong S-M, Muralidharan P, Jo SH, Kim DK (2010) One-step hydrothermal synthesis of CdTe nanowires with amorphous carbon sheaths. Mater Lett 64(14):1551–1554
32. Chua JH, Chee R-E, Agarwal A, Wong SM, Zhang G-J (2009) Label-free electrical detection of cardiac biomarker with complementary metal-oxide semiconductor-compatible silicon nanowire sensor arrays. Anal Chem 81(15):6266–6271
33. You HS, Choi KS, Bae PK, Kim KN, Jang HG, Kim Y-R, Kim CH (2009) Preparation and characterization of various surface-modified semiconductor nanocrystals. Notes 30(12):3137
34. Huang X-J, Choi Y-K (2007) Chemical sensors based on nanostructured materials. Sensors Actuators B Chem 122(2):659–671
35. Yoe JH, Jones AL (1944) Colorimetric determination of iron with disodium-1, 2-dihydroxybenzene-3, 5-disulfonate. Ind Eng Chem Anal Ed 16(2):111–115
36. Liu X-L, Zhu Y-J, Zhang Q, Li Z-F, Yang B (2012) Cd–cysteine precursor nanowire templated microwave-assisted transformation route to CdS nanotubes. Mater Res Bull 47(12):4263–4265
37. Parsons JG, Dokken KM, McClure J, Gardea-Torresdey JL (2013) FTIR, XAS, and XRD study of cadmium complexes with l-cysteine. Polyhedron 56:237–242
38. Monshi A, Foroughi MR, Monshi MR (2012) Modified Eq. 2 to estimate more accurately Nano-crystallite size using XRD. World J Nano Sci Eng 2:154
39. Pretsch E, Clerc T, Seibl J, Simon W (1989) Tables of spectral data for structure determination of organic compounds. Springer, Berlin, pp 205–210
40. Giusti MM, Wrolstad RE (2001) Characterization and measurement of anthocyanins by UV-visible spectroscopy. Current protocols in food analytical chemistry. Wiley, New York, pp 150–180
41. An X, Cao C, Yu X (2010) Fabrication of biocompatible Zn–cysteine nanowires and their application in selective fluorescence detection of Cu2+. J Nanosci Nanotechnol 10(12):8356–8361
42. Doak J, Gupta R, Manivannan K, Ghosh K, Kahol P (2010) Effect of particle size distributions on absorbance spectra of gold nanoparticles. Phys E Low-Dim Syst Nanostruct 42(5):1605–1609
43. Martinez CE, McBride MB (1998) Coprecipitates of Cd, Cu, Pb and Zn in iron oxides: solid phase transformation and metal solubility after aging and thermal treatment. Clay Clay Miner 46(5):537–545
44. Patoczka J, Johnson R, Scheri J (1998) Trace heavy metals removal with ferric chloride. In: Proceedings of Water Environment Federation Industrial Wastes Technical Conference, Nashville, TN. pp 1–14
45. Weerakkody NS, Caffin N, Lambert LK, Turner MS, Dykes GA (2011) Synergistic antimicrobial activity of galangal (Alpinia galanga), rosemary (Rosmarinus officinalis) and lemon iron bark (Eucalyptus staigerana) extracts. J Sci Food Agric 91(3):461–468
46. Kaloustian J, Portugal H, Pauli A, Pastor J (2002) Chemical, chromatographic, and thermal analysis of rosemary (Rosmarinus officinalis). J Appl Polym Sci 83(4):747–756
47. Huang N, Yang P, Leng Y, Chen J, Sun H, Wang J, Wang G, Ding P, Xi T, Leng Y (2003) Hemocompatibility of titanium oxide films. Biomaterials 24(13):2177–2187
48. Radojevic M, Bashkin VN (1999) Practical environmental analysis. Royal Society of Chemistry, London
49. Liang Z-Q, Wang C-X, Yang J-X, Gao H-W, Tian Y-P, Tao X-T, Jiang M-H (2007) A highly selective colorimetric chemosensor for detecting the respective amounts of iron (II) and iron (III) ions in water. New J Chem 31(6):906–910